Responding Phospholipid Membranes—Interplay between Hydration and Permeability

Emma Sparr and Håkan Wennerström
Division of Physical Chemistry 1, Center for Chemistry and Chemical Engineering, Lund University, SE-22100 Lund, Sweden

ABSTRACT Osmotic forces are important in regulating a number of physiological membrane processes. The effect of osmotic pressure on lipid phase behavior is of utmost importance for the extracellular lipids in stratum corneum (the outer part of human skin), due to the large gradient in water chemical potential between the water-rich tissue on the inside, and the relative dry environment on the outside of the body. We present a theoretical model for molecular diffusional transport over an oriented stack of two-component lipid bilayers in the presence of a gradient in osmotic pressure. This gradient serves as the driving force for diffusional motion of water. It also causes a gradient in swelling and phase transformations, which profoundly affect the molecular environment and thus the local diffusion properties. This feedback mechanism generates a nonlinear transport behavior, which we illustrate by calculations of the flux of water and solute (nicotine) through the bilayer stack. The calculated water flux shows qualitative agreement with experimental findings for water flux through stratum corneum. We also present a physical basis for the occlusion effect. Phase behavior of binary phospholipid mixtures at varying osmotic pressures is modeled from the known interlamellar forces and the regular solution theory. A first-order phase transformation from a gel to a liquid–crystalline phase can be induced by an increase in the osmotic pressure. In the bilayer stack, a transition can be induced along the gradient. The boundary conditions in water chemical potential can thus act as a switch for the membrane permeability.

INTRODUCTION

Diffusional motion is a main mechanism for molecular transport over mesoscopic distances (<100 μm). In the dynamic living state, water, small solute molecules, and macromolecules are transported within compartments but also across the barriers set by biological membranes. In a complex system, diffusional transport might deviate from a linear Fick's law description. It is well established that, in reacting systems with diffusion-controlled steps, one can have spontaneous spatial organizations (De Wit, 1999). Another possibility that has received less attention is that the gradients in concentration (or chemical potential) driving the diffusional motion also can cause phase changes, profoundly affecting the molecular environment and thus the local diffusion properties. This is a feedback mechanism leading to deviations from the linear Fick's law diffusion description.

In the present paper, we analyze a specific model where the diffusional motion of water is coupled to phase transformations across a stack of two-component phospholipid bilayers that separates two compartments with different chemical potential of water. Through a previous analysis of the equilibrium properties of the bilayer system at varying water chemical potential (Markova et al., 2000), we have the necessary background knowledge to analyze the phase behavior and the lamellar swelling in the water chemical potential established at steady state along the bilayer stack. This work is a continuation of a previous study of the transport over a stack of liquid–crystalline bilayers of negatively charged lipids (Sparr and Wennerström, 2000).

In a living system, the different compartments are typically separated by a membrane with a single lipid bilayer as the basic structural unit. There are, however, numerous exceptions where several bilayers are stacked, like in the myelin structure around nerve axones (Davis et al., 1999) and the membranes in retinal rods (Dratz and Hargrave, 1983). Landh (1996) gives several other examples of stacked bilayers in cell membranes. Clearly, stacking of bilayers will result in a decrease of molecular permeability.

One clear example of permeability reduction by bilayer stacking is found in the human skin. The outermost, thin layer of epidermis, stratum corneum, forms the main barrier for molecular diffusion through the skin, and it protects the body from uncontrolled water loss and uptake of hazardous chemicals from the environment. A stack of bilayers provides a solution to the problem of reducing the diffusional water flux through the skin driven by the relatively large gradient in water chemical potential from the blood to the ambient air. The stratum corneum is a 1–20-μm thick layer of dead cells (corneocytes) embedded in a lipid multilamellar matrix, where the bilayers are arranged parallel to the skin surface (Elias, 1991). The extracellular lipids constitute the only continuous regions of the stratum corneum, and molecules passing the skin barrier must be transported through the lipid domains (Potts and Francouer, 1990; Boddé et al., 1991). The lamellar organization of the lipids represents an almost ideal barrier to both strongly polar and strongly nonpolar substances, whereas those of intermediate polarity penetrate the skin more readily. Furthermore, it has been shown that the degree of hydration is strongly influencing the permeability of stratum corneum and model

Received for publication 13 December 2000 and in final form 21 April 2001.

Address reprint requests to Emma Sparr, Center for Chemistry and Chemical Engineering, Division of Physical Chemistry 1, Lund University, SE-22100 Lund, Sweden. Tel.: +46-46-222-32-48; Fax: +46-46-222-44-13; E-mail: emma.sparr@fkem1.lu.se.

0006-3495/01/08/1014/15 $2.00

membranes of stratum corneum lipids (Blank et al., 1984; Mandal and Downing, 1993).

Biological membranes typically contain a large number of different lipid species, and the permeability strongly depends on the physical state of the lipids. To understand the interplay between the lipid composition and the physical properties of the membrane, a large number of experimental and theoretical studies have been carried out on well-defined model lipid systems (Bloom et al., 1991; Cevc, 1993). It is well known that lipid mixtures can undergo phase segregation resulting from nonideal mixing of the lipids triggered by changes in thermodynamic conditions such as temperature, ionic strength, or osmotic pressure. This leads to lateral heterogeneity and the formation of domains of different chemical composition (Mouritsen and Jørgensen, 1997; Rietveld and Simons, 1998). In most biomembranes, the lipids are in the liquid–crystalline state under physiological conditions. However, in some cases, like for example the stratum corneum, the lipid bilayers are primarily in the crystalline state at ambient relative humidities and temperatures (Bouwstra et al., 1992), and only a smaller fraction of the lipids are suggested to be in the liquid–crystalline state (White et al., 1988; Hatcher and Plachy, 1993). According to the Domain Mosaic Model (Forslind, 1994) the lipid layers of stratum corneum can be envisioned as a mosaic of crystalline domains held together by lipids in a liquid–crystalline state.

In the majority of experimental work, lipid phase equilibria is studied in relation to variations in temperature. However, for many biological applications, it is equally relevant to consider the phase behavior at varying osmotic pressures (Π_{osm}) under isothermal conditions. In a few cases, $T - \Pi_{osm}$ phase diagrams for phospholipid–water systems have been established (Smith et al., 1990; Markova et al., 2000). One of the outcomes of these studies is that a first-order phase transformation from a liquid–crystalline to a gel phase can be induced by an increase in the osmotic pressure analogous to the temperature-induced transition in excess water. Osmotic forces are important in regulating a number of physiological membrane processes. For example, membrane fusion processes can be induced by creating a local osmotic stress (Hui et al., 1999). Another interesting example is cell injury caused by the freezing-induced dehydration of the lipid membranes in plants. In response to the increase in osmotic pressure, the plasma membranes of the leaves can go through a phase transformation into a reversed hexagonal phase, which induces massive leakage (Steponkus, 1999). The effect of osmotic pressure on lipid phase behavior is also of utmost importance in the case of human skin because of the large difference in water chemical potential present across the skin.

In this paper, we present a theoretical model for molecular diffusional transport over an oriented stack of two-component zwitterionic phospholipid bilayers in the presence of a gradient in water chemical potential, or equivalently, osmotic pressure. An essential feature of the model is the coupling between a steady-state flux of water and the thermodynamic response to the local water chemical potential. To determine the phase behavior of the zwitterionic lipids along the water gradient, we combine previous models for lipid–water systems (Guldbrand et al., 1982) and for lipid mixtures in excess solvent (Ipsen and Mouritsen, 1988). Phase transformations from liquid–crystalline bilayers, via two-phase coexistence bilayers, to gel bilayers are induced along the gradient in water chemical potential. The physical state of the lipids has very strong influence on the permeability of the membrane, which we illustrate by calculating the flux of water and solute through the bilayer stack. In the present paper, calculations were performed for two-component phospholipid membrane. This is not a representative system to model stratum corneum lipids, which include ceramides, cholesterol, and fatty acids but essentially no phospholipids (Wertz et al., 1987; Norlén et al., 1998). However, phospholipid systems are well studied and the large body of experimental data needed for making the numerical interpretations is available from the literature. As earlier described, it is well known that phospholipids can show a phase transition from a liquid–crystalline lamellar phase to a gel phase at increasing osmotic pressure of water. Similar phase behavior has also been demonstrated for extracted stratum corneum lipids (Gay et al., 1994) and for ceramides (Shah et al., 1995).

The paper is divided into four sections. First, we analyze the phase-equilibrium properties of homogeneous binary phospholipid mixtures at varying osmotic pressure. Then, we calculate the phase change in response to a gradient in osmotic pressure. This is followed by an analysis of the diffusional flux of water and of solutes.

PHASE EQUILIBRIA IN A HOMOGENOUS SYSTEM CONTAINING TWO PHOSPHOLIPID SPECIES

Free energy

In this section, we set out to calculate the phase equilibria of two-component homogenous mixtures of saturated phospholipids of different acyl-chain lengths at varying osmotic pressure. The major part of the composition-dependent free energy of a lamellar phase is due to the interlamellar interactions, G_{inter}, the free energy of mixing of the lipid species, G_{lip}, and lateral compression of the bilayers, G_{elast}. For a mixture of two lipids ($i = 1, 2$) at a given osmotic pressure (Π_{osm}) the total free energy can be written as a sum of G_{inter}, G_{lip}, G_{elast}, and the free energy of the standard states of the lipids, G^{θ},

$$\begin{aligned}\Delta G(n_1, n_2, \Pi_{osm}) &= G(n_1, n_2, \Pi_{osm}) - n_1 G_1^{\theta} - n_2 G_2^{\theta} \\ &= G_{inter}(n_1, n_2, \Pi_{osm}) + G_{lip}(n_1, n_2, \Pi_{osm}) \\ &\quad + G_{elast}(n_1, n_2, \Pi_{osm}), \qquad (1)\end{aligned}$$

where the fully swollen lamellar system, $\Pi_{osm} = 0$ is used as the standard state. In Eq. 1, n_i is the number of moles of lipid i. Here, G_{inter} can be obtained from the measured interbilayer force, F, by integration (Guldbrand et al., 1982),

$$G_{inter} = \int_h^\infty F \, dh. \quad (2)$$

As the water content, and the separation h, decreases, the bilayers increase slightly in thickness, or, equivalently, the area per lipid decreases. The elastic free energy, G_{elast}, associated with this deformation is relatively small for "stiff" bilayers with the high area expansion modulus typical for double-chain phospholipid systems (Lis et al., 1982b). As shown by Guldbrand et al. (1982), inclusion of the elastic contribution to the free energy only has a small influence on the phase equilibria, and, for simplicity, we will neglect this contribution below.

The free energy contribution from mixing the two lipids within the bilayers can be described by means of the regular solution theory,

$$\Delta G_{lip} = \sum_{i=1,2} RT \cdot n_i ln(X_i) + wX_1X_2, \quad (3)$$

where X_i is defined as mole fraction with respect to the total number of lipid molecules ($X_1 + X_2 = 1$). The last term in Eq. 3 represents the nonideal contribution to the mixing, where w is a single effective interaction parameter (Evans and Wennerström, 1999).

Chemical potentials

To model the phase diagram, we need a relation between Π_{osm} and X_i in the different phases. Equilibrium between two phases, α = I, II, requires that the chemical potentials of each component (water and lipids) are the same in all phases

$$\mu_w^I = \mu_w^{II} \quad and \quad \mu_i^I = \mu_i^{II}, \quad i = 1, 2. \quad (4)$$

The chemical potential of water is physically equivalent to the osmotic pressure for the solvent between the bilayers. The osmotic pressure between two planar parallel surfaces is simply the interaction force per unit area,

$$\Delta\mu_w = -V_w\Pi_{osm} = -V_w \frac{F}{area}, \quad (5)$$

where V_w is the molar volume of water. For zwitterionic phospholipids, an exponential short-range repulsive force dominates the interbilayer interaction (Rand and Parsegian, 1989; Israelachvili and Wennerström, 1992),

$$F_\alpha^r = F_\alpha^0 e^{-h_\alpha/\lambda_\alpha}. \quad (6)$$

The repulsive force is, at longer range, counterbalanced by an attractive force. The attractive dispersion force per area between two parallel sheets of thickness l interacting across water at a distance of h is given by

$$\frac{F_\alpha^a}{area} = -\frac{H}{6\pi}\left(\frac{1}{h_\alpha^3} - \frac{2}{(h_\alpha + l_\alpha)^3} + \frac{1}{(h_\alpha + 2l_\alpha)^3}\right) \quad (h > h_{min} \geq 0.2 \cdot 10^{-10}\text{m}) \quad (7)$$

(Parsegian et al., 1979), where H is the Hamacker constant. No other contributions to the surface interactions are considered, and the total force between the bilayers is expressed as the sum

$$F_\alpha = F_\alpha^r + F_\alpha^a. \quad (8)$$

At equilibrium, Eqs. 4 and 5 give

$$\mu_w^{II} - \mu_w^I = 0 \Leftrightarrow F_{II} - F_I = 0. \quad (9)$$

From Eqs. 6–9, the interlayer separation in phase I and II (h_I and h_{II}) can be calculated numerically for every value of $\Delta\mu_w$.

The next step is to calculate the chemical potential for the different lipids. This can be done by differentiating Eq. 1 with respect to the different species i. The chemical potential for lipid i in phase α is then equal to

$$\mu_i^\alpha = \mu_i^{\theta,\alpha} + \frac{A_\alpha}{2}\left\{\frac{G_{inter}^\alpha(h_\alpha)}{area} - h_\alpha \frac{F_\alpha(h_\alpha)}{area}\right\} + RT\ln(X_{i,\alpha}) + w_\alpha(1 - X_{i,\alpha})^2, \quad i = 1, 2 \quad \alpha = I, II, \quad (10)$$

where A_α is the average area per lipid headgroup in phase α. At equilibrium, the interlayer separations are determined by balancing the osmotic pressures, Eq. 9. From the equilibrium condition in Eq. 4 and the expression for the chemical potential (Eq. 10) applied to both lipid components, one obtains two equations for the compositions of the bilayers in the two coexisting phases (X_1 and X_2)

$$\Delta\mu_i^\theta = \mu_i^{\theta,II} - \mu_i^{\theta,I} = \frac{A_I}{2}\left\{\frac{G_{inter}^I(h_I)}{area} - h_I\frac{F_I(h_I)}{area}\right\} - \frac{A_{II}}{2}\left\{\frac{G_{inter}^{II}(h_{II})}{area} - h_{II}\frac{F_{II}(h_{II})}{area}\right\} + RT\ln\left(\frac{X_{i,I}}{X_{i,II}}\right) + w_I(1 - X_{i,I})^2 - w_{II}(1 - X_{i,II})^2, \quad i = 1, 2. \quad (11)$$

The difference in the standard chemical potential, $\Delta\mu_i^\theta$, of the lipid in phases I and II is strongly dependent on the temperature. For a sufficiently narrow temperature range, the enthalpy, H^θ, and the entropy, S^θ, can be considered as constants, and the difference in standard chemical potential can be expressed as

$$\Delta\mu_i^\theta = \mu_i^{\theta,II} - \mu_i^{\theta,I} \approx \Delta H_{i,I\to II}^\theta - T\Delta S_{i,I\to II}^\theta = (1 - T/T_{i,c})\Delta H_{i,I\to II}^\theta, \quad (12)$$

TABLE 1 Parameters used in the calculations; Transition enthalpies, transition temperatures at excess water, and bilayer thickness for DMPC, DLPC, and DPPC (Cevc, 1993)

	DLPC	DMPC	DPPC
$\Delta H_{L_\beta \to P_\beta}$ (kJ/mol)		5	7.5
$\Delta H_{P_\beta \to L_\alpha}$ (kJ/mol)		26	36.5
$\Delta H_{L_\beta \to L_\alpha}$ (kJ/mol)	18	(31)	(44)
$T_{c,L_\beta \to P_\beta}$ (°C)		14	34
$T_{c,P_\beta \to L_\alpha}$ (°C)		23.5	41.5
$T_{c,L_\beta \to L_\alpha}$ (°C)	−1	(21.5)	(40)
I_{L_α} (Å)	42	45	47
I_{P_β} (Å)		46	48
I_{L_β} (Å)	34	38	41

Values in parenthesis correspond to the metastable L_β–L_α transition in excess water.

where $T_{i,c}$ is the phase transition temperature for the pure lipid in excess water.

By combining Eqs. 9, 11, and 12, relations between X_I, X_{II}, h_I, and h_{II} are obtained for a given temperature T. The interlamellar separations in each phase, h_I, h_{II}, at a given osmotic pressure, Π_{osm}, are determined from Eqs. 5–9. Consequently, the composition of the different phases, X_I and X_{II}, can be calculated for every value of the osmotic pressure, Π_{osm}.

In the numerical calculations, we assume that the amplitude (F_α^0) and the decay lengths (λ_α) of the repulsive force is only determined by the phase state and is independent of the exact composition of the bilayers. For simplicity, the change in the attractive force due to changes in lipid bilayer thickness is also neglected as this has a negligible influence on the resulting force in the range of separations studied. Consequently, the interaction force is determined by the physical state of the lipids only. This assumption is justified by experimental force measurements showing that, in the relevant separation range, the interaction force is within the experimental accuracy independent of small variations in acyl chain lengths as long as the lipids are in the same state (Lis et al., 1982a; Markova et al., 2000).

The exponential repulsive force has been monitored for L_β and L_α phases (Lis et al., 1982a; Markova et al., 2000). Numerical values of F_0^α and λ_α for these phases can be obtained from the exponential curve fit to osmotic stress data (Lis et al., 1982a). No experimental results describing the interaction force in the P_β phase are available from the literature. To obtain a consistent picture, the amplitude of the repulsive force, $F_0^{P_\beta}$, is adjusted so that the experimentally determined distances at maximum swelling are reproduced. The decay length, λ_{P_β}, is chosen to be intermediate to the decay length for the L_β and the L_α phases (Guldbrand et al., 1982). The Hamacker constant for lipid–water–lipid is set to $H = 6.0 \times 10^{-21}$ J, which is typical for hydrocarbon–water systems (Israelachvili, 1992). Parameters used for the numerical calculations are summarized in Table 1 and 2.

For the numerical treatment of the nonideal case, the effective interaction parameter, w, is required. Ipsen and Mouritsen (1988) have proposed a model based on a regular solution theory to describe equilibria in two-component phospholipid bilayers in excess water. This model shows a good agreement with experimental results (Shimshick and McConnell, 1973). We assume the interaction parameter to be independent of the water content, and the effective interaction parameter obtained by Ipsen and Mouritsen (1988) for excess water is used.

TABLE 2 Parameters used in the calculations. Amplitude and decay length of the exponential repulsive force and the average area per lipid headgroup in the different phases $\alpha = L_\alpha$, L_β, and P_β

	L_α	L_β	P_β
F_α^0/area (N/m^2)	1.3×10^9	6.8×10^8	1.3×10^9
λ_α (Å)	2.2	2.0	2.1
A_α (Å^2)	57	49	49

Phase equilibria

Most experimental studies of phospholipid phase equilibria have been made for systems with an excess of pure water, implying $\Pi_{osm} = 0$. With a limited supply of water, a new thermodynamic degree of freedom manifests itself. For a system of one phospholipid and water, a binary the T–X_w diagram has been used to represent the phase equilibria (Ulmius et al., 1977; Janiak et al., 1979; Gabriella-Madelmont and Perron, 1983). An alternative procedure is to control the osmotic pressure at a constant nonzero level, leading to a T–Π_{osm} representation (Smith et al., 1990; Markova et al., 2000). One outcome of these studies is that a transition from gel to the liquid–crystalline phase can be induced by an increase in water chemical potential, analogous to the transition induced by an increase in temperature in excess water.

In this work, the phase equilibria in binary phospholipid–water mixtures are modeled at varying osmotic pressure and isothermal conditions. Calculations were performed for saturated phospholipids of different chain lengths [DLPC (dilauroyl phosphatidyle choline, C12:0), DMPC (dimyristoyl phosphatidyl choline, C14:0), DPPC (dipalmitoyl phosphatidyl choline, C16:0)], and the L_β–L_α, L_β–P_β, and P_β–L_α phase transitions are considered. The calculated phase diagram for DLPC–DMPC, 30°C is shown in Figure 1 *A*. At this temperature, the single phospholipid–water systems go through the transitions from gel (L_β) to liquid crystalline (L_α) phase at 75% relative humidity (RH) (DLPC) and 90%RH (DMPC), respectively. In the phase diagram for the binary phospholipid mixture, the L_α, L_β, or coexisting, L_α/L_β, phases are present. The phase diagram for DLPC–DPPC, 30°C is shown in Figure 1 *B*. This phase diagram differs from the previous one because DPPC at 30°C is in the L_β state over the whole range of osmotic pressure and does not reach the hydration melting limit. The

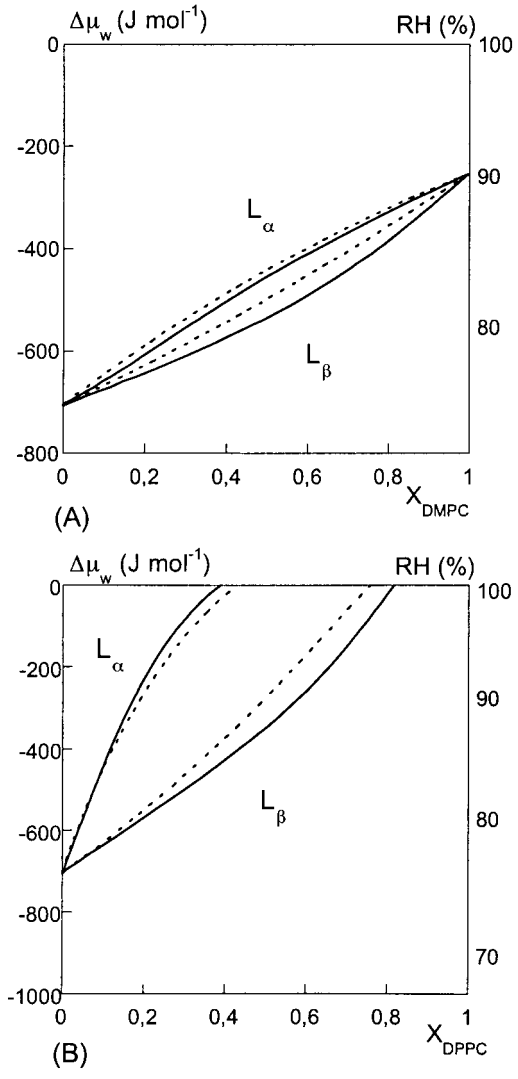

FIGURE 1 Calculated phase $\Delta\mu_w$–X diagram for (*A*) DLPC–DMPC mixtures, 30°C and (*B*) DLPC–DPPC mixtures, 30°C. Dotted lines give the phase boundaries for the ideal system ($w = 0$), solid lines give the phase boundaries for the nonideal system ($w_{L_\alpha} = 1.4$ kJ/mol, $w_{L_\beta} = 1.7$ kJ/mol) (Ipsen and Mouritsen, 1988). *Left-hand axis:* the chemical potential of water, $\Delta\mu_w$. *Right-hand axis:* the corresponding relative humidity, RH ($RH = \exp(\Delta\mu_w/RT)$).

dotted lines in the phase diagrams give the phase boundaries for the ideal systems ($w = 0$, Eq. 3), whereas the solid lines represent the phase boundaries for the gel–liquid-crystal transition where the nonideal interactions are taken into account ($w \neq 0$, Eq. 3). It can be noted that the nonideality induces an asymmetry of the two-phase regions, where the deviations from the ideal behavior are more distinct in the gel phase.

Phase behavior of binary phospholipid mixtures in excess water has been extensively studied both experimentally and theoretically (Shimshick and McConnell, 1973; Mabrey and Sturtevant, 1976; Engelbert and Lawaczeck, 1985; Ipsen and Mouritsen, 1988; Sugar et al., 1999). It has been demonstrated that the nonideal behavior is more pronounced at increasing difference of the acyl-chain lengths. It has also been observed that the miscibility is lower in the gel phase. Phase transitions triggered by changes in osmotic pressure have received much less attention, and no experimental phase diagrams of this kind can be found in the literature. One of the most striking observations from the calculated phase diagrams in Fig. 1 is that the osmotic pressure-induced phase behavior closely resembles the corresponding thermally induced phase behavior (Shimshick and McConnell, 1973; Ipsen and Mouritsen, 1988). This shows that similar effects on the phase behavior can be achieved by varying different intensive variables.

The phase behavior of the binary phospholipid–water mixtures is, of course, also strongly dependent on the temperature. Figure 2, *A–C*, shows the progression of the phase boundaries in the DMPC–DPPC phase diagram as the temperature moves. As a guide for the interpretations of these phase diagrams, the schematic $T - \Delta\mu_w$ phase diagram for the single phospholipid–water mixture is shown in Fig. 2 *D* (Markova et al., 2000). The qualitative phase diagrams for these phospholipids of different chain lengths are very similar, with the main difference being a translation along the temperature axis. DPPC is in the L_β state over the whole range of osmotic pressure at temperatures below 34°C. For $T < 21.5$°C (DMPC pretransition ($L_\beta \rightarrow P_\beta$), Figure 2 *D*), the L_β phase is present at all compositions and osmotic pressures. For $21.5°C < T < 23.5°C$, a P_β phase is induced in the DMPC-rich mixtures (figure not shown) and, for $23.5°C < T < 26°C$, both the P_β and L_α phases are present over a rather wide range of compositions (Fig. 2 *A*). At $T >$ 26°C (DMPC three-phase point, Fig. 2 *D*), the single DMPC–water system goes through the chain melting transition $L_\beta \rightarrow L_\alpha$ without passing the P_β phase. Figure 2 *B* shows the DMPC–DPPC phase diagram for $T = 30$°C. At this temperature, the P_β phase is not formed in any of the single phospholipid–water mixtures at any osmotic pressure. However, in the binary bilayers, the P_β phase is induced. In the phase diagram, a three-phase line is connecting the different phases at a constant osmotic pressure corresponding to $\Delta\mu_w = 140$ J/mol (Fig. 2 *B*). As the temperature further increase, the phase boundaries move toward higher fractions of DPPC, and, finally, DPPC goes through the transition into the P_β phase (Fig. 2 *C*) and L_α phase (figure not shown). At $T > 45$°C (DPPC three-phase point, Fig. 2 *D*) the phase diagram looks qualitatively the same as the DLPC–DMPC phase diagram in Fig. 1 *A*.

PHASE EQUILIBRIA IN THE PRESENCE OF A GRADIENT IN WATER–CHEMICAL POTENTIAL

System

Consider N parallel ordered bilayers of a binary mixture of zwitterionic phospholipids (Fig. 3). The phospholipid com-

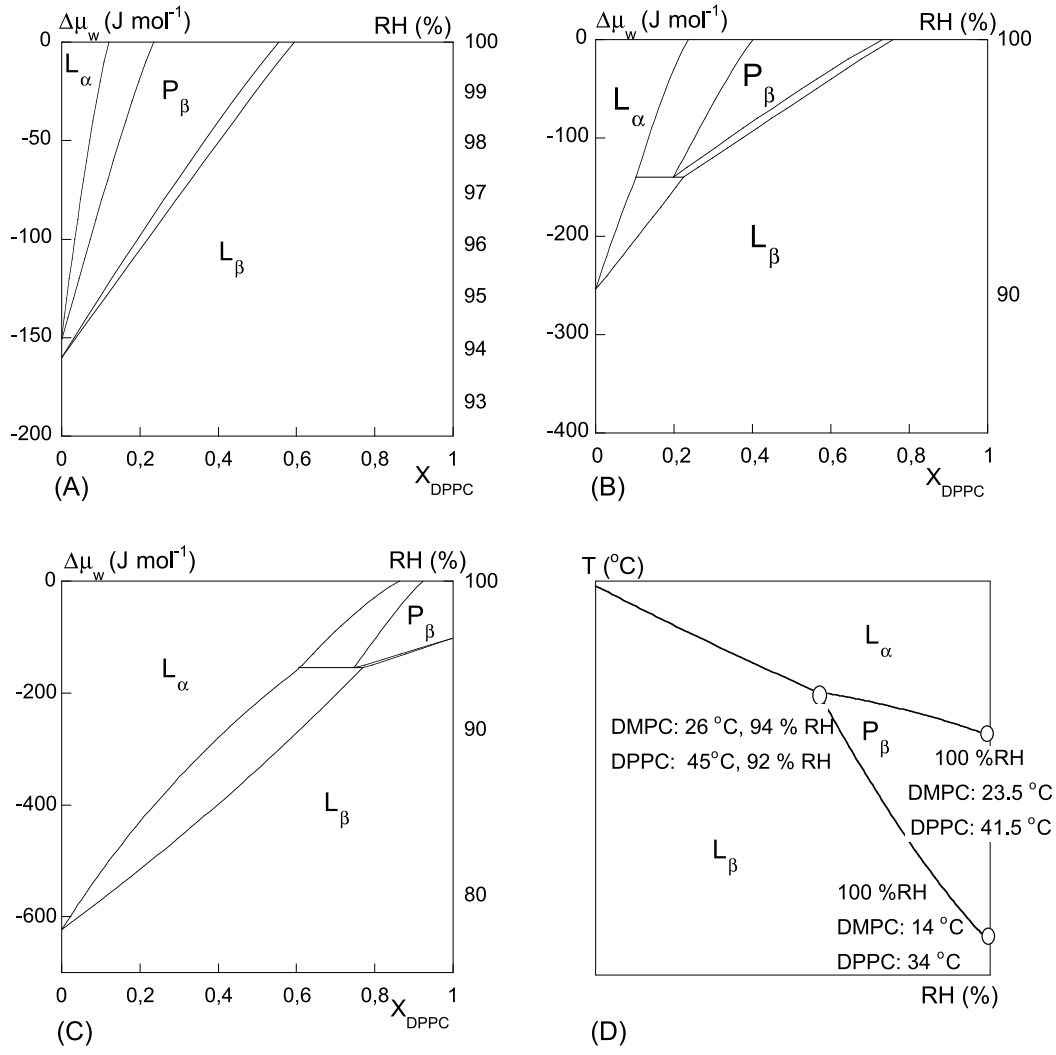

FIGURE 2 Calculated phase $\Delta\mu_w$–X diagram for DMPC–DPPC mixtures at (*A*) 25°C, (*B*) 30°C and (*C*) 40°C. *Left-hand axis:* the chemical potential of water, $\Delta\mu_w$. *Right-hand axis:* the corresponding relative humidity, RH (RH = $\exp(\Delta\mu_w/RT)$). To facilitate the interpretation of the diagrams (*A–C*), the T–$\Delta\mu_w$ phase diagrams of the single phospholipid–water mixtures is shown in (*D*) (Markova et al., 2000). The phase behavior of the DMPC–water and DPPC–water systems mainly differs by a translation along the temperature axis. Temperatures and relative humidities at the pretransition, L_β–P_β in excess water, the main transition, P_β–L_α in excess water and the three-phase-point P_β–L_β–L_α are indicated in the figure.

position X_1 is assumed to be the same in all bilayers. On the upper side ($z = W$), the stack is exposed to air with a specified RH, and the boundary condition of water chemical potential is given by $\Delta\mu_w^{rh} = RT \ln(RH)$. On the lower side ($z = 0$), the water chemical potential is fixed to $\Delta\mu_w^{ref} = \mu_w^{ref} - \mu_w^0$, representing a reference state of bulk solution. In the calculations, we are using physiological saline solution to represent the reference state at $z = 0$, corresponding to RH ≈ 99.5%. Every layer in the stack can be regarded as a discrete unit consisting of two separated domains, the lipid bilayer and the aqueous interlamellar layer. Along the gradient, the lipid phase behavior and the aqueous layer swelling vary with the local chemical potential of water. We assume a high thermal conduction so that the temperature is uniform throughout the system.

Swelling and phase transformations

In a previous paper, we have presented a model for molecular diffusion through a stack of charged lipid bilayers in the liquid crystalline state (Sparr and Wennerström, 2000), where the interlamellar force is dominated by the electrostatic repulsion. For the system consisting of zwitterionic lipids, an exponential short-range repulsive force is dominating the interaction. We assume that the expression for swelling at equilibrium can also be applied at the steady-state conditions. This implies that the variation in lipid phase behavior along the gradient in water chemical potential, $\Delta\mu_w$, can be calculated on the basis of the local surface forces between the lamellae and from the thermodynamic properties of the lipids. According to the phase diagrams

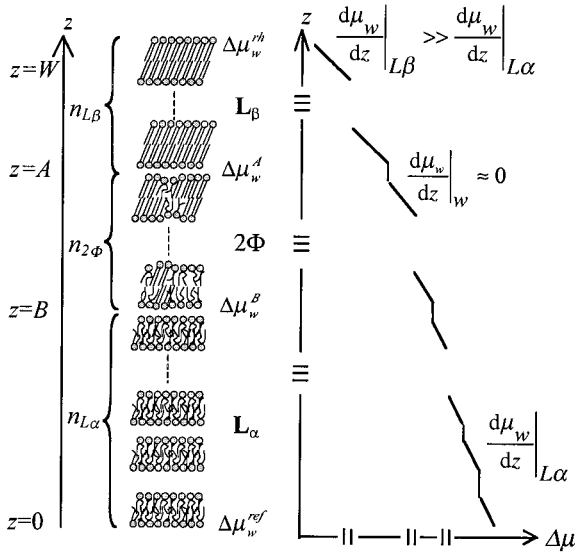

FIGURE 3 Schematic representation of a binary phospholipid bilayer stack in the presence of water chemical potential, $\Delta\mu_w$. On the lower side of the stack ($z = 0$), the chemical potential, $\Delta\mu_w^{ref}$, corresponds to a physiological saline solution. On the upper side ($z = W$), the boundary condition, $\Delta\mu_w^{rh}$, is determined from the relative humidity of air. Along the gradient in $\Delta\mu_w$, the lipid bilayers go through transformations from liquid–crystalline (L_α) to gel (L_β) state via a two-phase coexistence (2Φ) region. The transitions occur at $\Delta\mu_w = \Delta\mu_w^B$ (L_α–2Φ) and at $\Delta\mu_w = \Delta\mu_w^A$ (2Φ–L_β) at $z = A$, B, respectively. The number of bilayers is denoted N, and the number of bilayers in each state are n_{L_α}, $n_{2\Phi}$, and n_{L_β}. The gradient in $\Delta\mu_w$ is much larger over the gel state bilayers than over the liquid crystalline bilayers. In the aqueous layers, the gradient in $\Delta\mu_w$ is approximately zero.

described in the previous section, we can then expect a variation in phase behavior along the gradient.

For clarity, we have chosen to describe the case where the equilibrium phase behavior corresponds to the phase diagram in Fig. 1 *A*, i.e., when a two-phase region separates the L_β and L_α regions, and no P_β phase is present. This does not cause any restriction to the general description because the transitions to the P_β phase can be treated in an analogous manner to the L_β–L_α transition. The phase transitions from a gel to a liquid–crystalline phase along the gradient has a profound effect on the permeabilities of water and solutes through the bilayers, whereas the effect of the transition between two different gel phases is expected to be much smaller.

In the following sections, we will treat the case for which lamellar phase is in a liquid–crystalline state (L_α) at the water chemical potential of $\Delta\mu_w^{ref}$, i.e., at the lower boundary ($z = 0$). The membrane properties can then be investigated for varying boundary conditions $\Delta\mu_w^{rh}$. If the system is chosen so that the bilayers are in gel state (L_β) at the water chemical potential of $\Delta\mu_w^{rh}$, i.e., at the upper boundary ($z = W$), a two-phase liquid-crystalline–gel region will be present along the gradient at water chemical potentials in the range of $\Delta\mu_w^A < \Delta\mu_w < \Delta\mu_w^B$ (see Fig. 3).

Besides the phase transitions, the lamellar stack will also respond to the local water chemical potential by a nonhomogenous swelling along the gradient. This swelling can be calculated from the experimentally determined interlamellar forces in the different phases (Eqs. 6 and 7). We assume that the probability for the "perpendicular" interactions between the L_β–L_β, L_α–L_α, and L_α–L_β phases in the two-phase region can be determined from the product of the area fractions of the different phases and that the resulting force is additive,

$$F_{2\Phi} = \frac{(X_{L_\alpha}A_{L_\alpha})^2F_{L_\alpha} + 2(X_{L_\alpha}A_{L_\alpha})(X_{L_\beta}A_{L_\beta})F_{L_\alpha-L_\beta} + (X_{L_\beta}A_{L_\beta})^2F_{L_\beta}}{(X_{L_\alpha}A_{L_\alpha} + X_{L_\beta}A_{L_\beta})^2}. \quad (13)$$

In analogy with the derivation for the Hamacker constant in mixed systems, the amplitude of the repulsive interaction between two bilayers in different states is calculated as $F^0_{L_\alpha-L_\beta} = \sqrt{F^0_{L_\alpha}F^0_{L_\beta}}$ and the decay length, $\lambda_{L_\alpha-L_\beta}$ is assumed to be intermediate to λ_{L_α} and λ_{L_β}. The assumptions made for the interaction force in the two-phase bilayers is not critical to the final results because the swelling effect in these regions is not so dramatic.

WATER FLUX

Steady-state water flux through a bilayer stack

As a consequence of the gradient in $\Delta\mu_w$ ($\Delta\mu_w^{rh} \neq \Delta\mu_w^{ref}$), water will diffuse through the lamellar system. In a multilamellar stack, the local concentration of water is orders of magnitude larger in the aqueous domains than in the bilayers, and the diffusion of water is thus much more efficient there. The gradient in $\Delta\mu_w$ across the aqueous part is consequently negligibly small, and the whole gradient in $\Delta\mu_w$ is, to a good approximation, located to the lipid regions (Fig. 3). This implies that the steady-state water flux is independent of the swelling of the aqueous layers and is only determined from the state and thickness of the lipid bilayers and from the boundary conditions (Sparr and Wennerström, 2000). The water flux across the one-phase bilayers in L_α and L_β state can thus be calculated from Fick's first law of diffusion by integration over the lipid regions (cf. Sparr and Wennerström, 2000, Eq. 7)

$$\begin{aligned} J_{w,L_\alpha} &= -\frac{D_w^{L_\alpha}c_0^{L_\alpha}}{n_{L_\alpha}l_{L_\alpha}}(c_w^{L_\alpha}(B) - c_w^{L_\alpha}(0)) \\ &= -\frac{D_w^{L_\alpha}c_{w,0}^{L_\alpha}}{n_{L_\alpha}l_{L_\alpha}}(e^{\Delta\mu_w^B/RT} - e^{\Delta\mu_w^{ref}/RT}), \\ J_{w,L_\beta} &= -\frac{D_w^{L_\beta}c_0^{L_\beta}}{n_{L_\beta}l_{L_\beta}}(c_w^{L_\beta}(W) - c_w^{L_\beta}(A)) \\ &= -\frac{D_w^{L_\beta}c_{w,0}^{L_\beta}}{n_{L_\beta}l_{L_\beta}}(e^{\Delta\mu_w^{rh}/RT} - e^{\Delta\mu_w^A/RT}). \end{aligned} \quad (14)$$

In Eq. 14, n_α is the number of bilayers in phase α, $\alpha = L_\alpha, L_\beta$ (see Fig. 3). $c^\alpha_{w,0}$ and $c^\alpha_w(z)$ are the water concentrations in the lipid bilayer in equilibrium with pure water and with water at position z, respectively, and D^α_w is the diffusion coefficient for water in the hydrocarbon parts of the bilayers.

When describing the water flux through the two-phase bilayers, two parallel flux have to be considered; that is, the water flux through the liquid crystalline parts, $J_{2\Phi,L_\alpha}$, and the water flux through the gel parts, $J_{2\Phi,L_\beta}$, of each bilayer. An additional constraint is that the water chemical potential has to be constant at the bilayer–aqueous interface of each bilayer independent of the state of the lipids. The water flux over bilayer number n is then determined from the flux through the gel and liquid crystalline domains of the bilayer, weighted by the area fraction of each phase,

$$J_{2\Phi}(n) = \frac{A_{L_\alpha}X_{L_\alpha}(n)J_{2\Phi,L_\alpha}(n) + A_{L_\beta}X_{L_\beta}(n)J_{2\Phi,L_\beta}(n)}{A_{L_\alpha}X_{L_\alpha}(n) + A_{L_\beta}X_{L_\beta}(n)}. \tag{15}$$

The fractions of the different phases, $X_\alpha(n)$, in layer n are determined by the local water chemical potential and the lever rule. The flux over the different domains, $J_{2\Phi,L_\alpha}(n)$ and $J_{2\Phi,L_\beta}(n)$ can be expressed by Fick's first law of diffusion, and Eq. 15 can be rewritten as

$$J_{2\Phi} = -\frac{A_{L_\alpha}X_{L_\alpha}\dfrac{D^{L_\alpha}_w c^{L_\alpha}_0}{l_{L_\alpha}}e^{\Delta\mu_w/RT} + A_{L_\beta}X_{L_\beta}\dfrac{D^{L_\beta}_w c^{L_\beta}_0}{l_{L_\beta}}e^{\Delta\mu_w/RT}}{A_{L_\beta}X_{L_\alpha} + A_{L_\beta}X_{L_\beta}}\frac{d\mu_w}{dn}, \tag{16}$$

where $0 \le n \le n_{L_{2\Phi}}$ and $\Delta\mu^A_w < \Delta\mu_w \le \Delta\mu^B_w$ (Fig. 3). $n_{L_{2\Phi}}$ is the number of two-phase bilayers. The differential equation in Eq. 16 can be solved numerically to give the steady-state flux over the two-phase bilayers as a function of the boundary conditions, $\Delta\mu^{rh}_w$.

At steady state, the flux is independent of the position, and the total flux must be equal to the water flux through each region of the bilayer stack, that is $J = J_{L_\alpha} = J_{2\Phi} = J_{L_\beta}$. Consequently, Eqs. 14 and 16, together with total number of bilayers in the stack,

$$N = n_{L_\alpha} + n_{2\Phi} + n_{L_\beta}, \tag{17}$$

are conditions enough to give a solution for the water flux over the whole stack. It should be noted that the area per lipid headgroup, A_α, is not the same in the gel and the liquid–crystalline phases. This implies that the total area of the bilayers change along the gradient in $\Delta\mu_w$. In the present work, we treat the flux per area, and it is therefore sufficient to consider only the variations in area fraction of each phase along the gradient. However, if determining the total flow over the membrane, the changes in the total area have to be taken into account. Furthermore, small variations in area compression upon hydration have been observed in the L_α and L_β bilayers (Lis et al., 1982b). At the present stage, this effect is neglected because it only causes small quantitative changes of the final results.

Water chemical potential

The total gradient in the water chemical potential is the sum over the gradients in water chemical potential over every layer n. The variations in chemical potential along the bilayer stack can be expressed in the profile, $n(\Delta\mu_w)$, specifying the layer number for a given $\Delta\mu_w$. At a certain boundary condition, $\Delta\mu^{rh}_w$, the numbers of bilayers in each state, $n_{L_\alpha}(\Delta\mu^{rh}_w)$, $n_{2\Phi}(\Delta\mu^{rh}_w)$, and $n_{L_\beta}(\Delta\mu^{rh}_w)$ can be obtained from Eqs. 14, 16, and 17. Having determined the steady-state flux for a given $\Delta\mu^{rh}_w$, we can determine the drop in water chemical potential per bilayer from the known permeability of the respective phases. In this way, we can calculate the chemical potential profile $n(\Delta\mu_w)$ ($\Delta\mu^{rh}_w \le \Delta\mu_w \le \Delta\mu^{ref}_w$),

$$n(\Delta\mu_w) = \begin{cases} n_{L_\alpha}(\Delta\mu^{rh}_w)\dfrac{e^{\Delta\mu_w/RT} - e^{\Delta\mu^{ref}_w/RT}}{e^{\Delta\mu^B_w/RT} - e^{\Delta\mu^{ref}_w/RT}}, & \Delta\mu^B_w < \Delta\mu_w \le \Delta\mu^{ref}_w, \\ n_{L_\alpha}(\Delta\mu^{rh}_w) + n_{2\Phi}(\Delta\mu^{rh}_w) \\ \quad \times \dfrac{\int_{\Delta\mu^B_w}^{\Delta\mu_w}(X_{L_\alpha}(\Delta\mu_w)P_{L_\alpha} + X_{L_\beta}(\Delta\mu_w)P_{L_\beta})e^{\Delta\mu_w/RT}d\mu_w}{\int_{\Delta\mu^B_w}^{\Delta\mu^A_w}(X_{L_\alpha}(\Delta\mu_w)P_{L_\alpha} + X_{L_\beta}(\Delta\mu_w)P_{L_\beta})e^{\Delta\mu_w/RT}d\mu_w}, \\ \qquad\qquad \Delta\mu^A_w < \Delta\mu_w \le \Delta\mu^B_w, \\ n_{L_\alpha}(\Delta\mu^{rh}_w) + n_{2\Phi}(\Delta\mu^{rh}_w) \\ \quad + n_{L_\beta}(\Delta\mu^{rh}_w)\dfrac{e^{\Delta\mu_w/RT} - e^{\Delta\mu^A_w/RT}}{e^{\Delta\mu^{rh}_w/RT} - e^{\Delta\mu^A_w/RT}}, & \Delta\mu_w \le \Delta\mu^A_w. \end{cases} \tag{18}$$

When $\Delta\mu^{rh}_w \ge \Delta\mu^B_w$, i.e., all the bilayers in the stack are L_α phase, only the upper form in Eq. 18 is relevant. For $\Delta\mu^{rh}_w < \Delta\mu^B_w$, parts of the bilayers have two coexisting phases where the relative proportion varies so that the effective permeabilities change. This gives a clearly nonlinear relation between n and $\Delta\mu_w$. When $\Delta\mu^{rh}_w < \Delta\mu^A_w$, the upper bilayers (large $n \le N$) are in the one-phase L_β state, which implies a simple change in $\Delta\mu_w$ for each unit change in n.

A relation between the water chemical potential, $\Delta\mu_w$, and the vertical placement, $z(n)$, can be obtained by including the swelling of the lamellar phase along the gradient

$$z(n) = \sum_{i=1}^{n}(l_\alpha(i) + h_\alpha(i)). \tag{19}$$

In Eq. 19, $h_\alpha(n)$ is the thickness of interlayer aqueous spacing and $l_\alpha(n)$ is the (average) thickness of the bilayer in layer n, $\alpha = L_\alpha$, 2Φ, L_β. For large values of n, Eq. 19 can be interpreted as a Riemann sum of a continuous function, and the expression can be turned into an integral to give a continuous function for the $z(\Delta\mu_w)$ profile

$$z(\Delta\mu_w) = \int_0^n [l(\Delta\mu_w(n)) + h(\Delta\mu_w(n))]\,dn$$

$$= \int_{\Delta\mu_w^{ref}}^{\Delta\mu_w} [l(\Delta\mu_w) + h(\Delta\mu_w)] \frac{dn(\Delta\mu_w)}{d\mu_w}\,d\mu_w, \quad (20)$$

where $n(\Delta\mu_w)$ is given in Eq. 18.

If $n = N$ (i.e., all layers), Eq. 20 can be rewritten to give the variation in the total thickness of system as a function of the relative humidity at the boundary,

$$W(\Delta\mu_w^{rh}) = \int_0^N [l(\Delta\mu_w(n)) + h(\Delta\mu_w(n))]\,dn$$

$$= \int_{\Delta\mu_w^{ref}}^{\Delta\mu_w^{rh}} [l(\Delta\mu_w) + h(\Delta\mu_w)] \frac{dn(\Delta\mu_w)}{d\mu_w}\,d\mu_w. \quad (21)$$

Water flux through a responding lipid membrane

One of the major functions of biological membranes is to regulate the permeability of water and other chemical species. In this work, responding membranes of phospholipid bilayers are studied. In the following section, we have chosen to illustrate the general results with calculations for the specific system of a DLPC–DMPC ($X_{DLPC} = 0.5$) membrane at 30°C. For this system, we find $\Delta\mu_w^A = -535$ J/mol (80%RH) and $\Delta\mu_w^B = -455$ J/mol (83%RH), and the fraction of each phase along the gradient in $\Delta\mu_w$ is obtained from the phase diagram in Fig. 1 *A* (nonideal case). In the numerical calculations, the number of layers was set to $N = 1000$. The lipid bilayer thicknesses in the L_α and L_β phases are summarized in Table 1. The thickness of the binary lipid bilayers is calculated as the weighted average thickness of each phase.

The water flux across the stack of lamellae is determined from the boundary conditions, the state of the lipids and the number of bilayers. Figure 4 shows the water flux calculated from Eqs. 14, 16, and 17. For boundary conditions of $\Delta\mu_w^{rh} > \Delta\mu_w^B$, the whole stack is in the liquid–crystalline state and the flux varies linearly with RH%. When the boundary conditions of water chemical potential decreases below $\Delta\mu_w^B$ a fraction of the upper bilayers will transform into a gel state. The permeability in the gel phase is much lower than in the liquid–crystalline phase (Lawaczeck, 1979). Consequently, the permeability of the membrane is considerably reduced as the fraction of the gel phase is increased. This can be seen as the leveling off in the flux curve at $\Delta\mu_w^{rh} = \Delta\mu_w^B$. When the whole upper bilayer is in the gel state, $\Delta\mu_w^{rh} < \Delta\mu_w^A$, the calculated flux shows a virtual independence of the relative humidity.

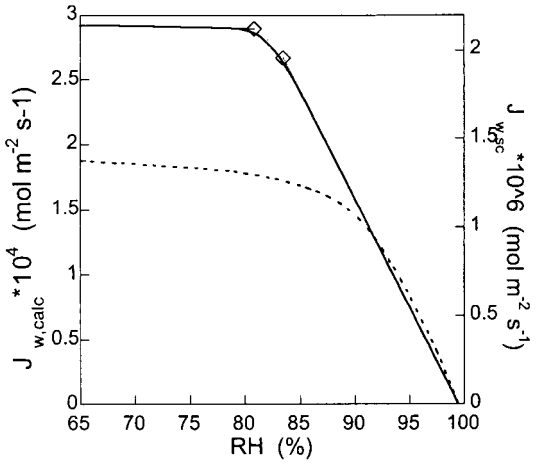

FIGURE 4 Water flux as a function of the relative humidity at the boundary. *Solid line:* Calculated profile for DLPC–DMPC ($X_{DMPC} = 0.5$) membrane (*left-hand axis*). The diamonds indicate where the upper bilayer goes through the transitions; (L_α–2Φ) at $\Delta\mu_w^B = -455$ J/mol (83%RH) and (2Φ–L_β) at $\Delta\mu_w^A = -535$ J/mol (80%RH). $T = 30$°C, $P_{H_2O}^{L_\alpha} = 3 \times 10^{-5}$ m/s, $P_{H_2O}^{L_\beta} = 3 \times 10^{-7}$ m/s, $N = 1000$. *Dotted line:* Experimental water flux (per area stratum corneum) from Blank et al. (1984). (*right-hand axis*).

The calculated water flux shows a nonlinear response to the boundary condition in water chemical potential. A qualitatively similar response to the boundary condition of relative humidity is also observed for water flux through stratum corneum. The dotted line in Fig. 4 represents experimental data for water flux through stratum corneum obtained by Blank et al. (1984). When comparing the curves in Fig. 4, it is important to note that the relative humidity at which the curve starts to level off is purely determined by the properties of the particular lipid system. However, the described mechanism is generally applicable. The response to changes in gradient in water chemical potential of the experimental water flux in stratum corneum is qualitatively consistent with the response of the calculated flux, suggesting that the mechanism described in the present model is also a mechanism operating for the skin lipids.

It can be noted that the calculated flux is about two orders of magnitude higher than the experimental flux through stratum corneum (Fig. 4). In the calculations, the permeability of water in a liquid–crystalline lipid bilayer was set to 3×10^{-5} m/s (Graziani and Livne, 1972) and the permeability in a gel bilayer was assumed to be 100 times lower. The numbers of layers was set to $N = 1000$. The choice of these parameters is, of course, crucial for the exact values of the flux. The calculated flux should therefore be seen as a qualitative result, rather than quantitative values of

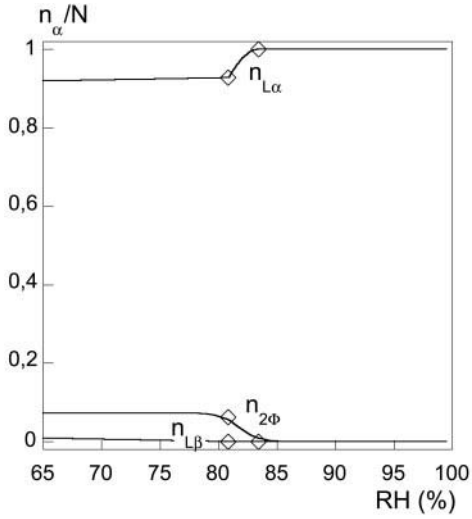

FIGURE 5 The fraction of bilayers in the different state (n_{L_α}/N, $n_{2\Phi}/N$, and n_{L_β}/N) in a DLPC–DMPC ($X_{DMPC} = 0.5$) membrane as a function of the relative humidity at the boundary. The diamonds indicate $\Delta\mu_w^A$ and $\Delta\mu_w^B$ phase boundaries where the upper bilayer goes through the transitions (L_α–2Φ) and (2Φ–L_β) ($T = 30°C$).

the water flux. In comparison with the flux through stratum corneum, we have, in particular, neglected the presence of corneocytes and the crystalline fraction of the lipids, which are expected to lower the effective permeability (Falla et al., 1996; Forslind, 1994; Kitson and Thewalt, 2000).

From Eqs. 14, 16, and 17 the number of bilayers in each state at varying boundary conditions of relative humidity can be calculated. Figure 5 shows how $n_{L\alpha}$, $n_{2\Phi}$, and $n_{L\beta}$ vary with RH%. A striking observation from the figure is that only a very small fraction of bilayers are in the L_β state. The steady-state flux is independent of the vertical position along the stack and a reduced permeability is then balanced by a larger gradient over fewer layers. It is worth noting that the presence of a small number of gel bilayers has a strongly reducing effect on the effective permeability of the membrane (Fig. 4).

Swelling of a responding lipid membrane

The water-layer swelling along the gradient is determined from the repulsive force between the bilayers. A straightforward consequence of the gradient in swelling is that the total thickness of the system varies with changes in boundary conditions. The swelling is most pronounced for high humidities, whereas, for lower relative humidities, the thickness of the stack approaches a nearly constant value of ≤60% of the fully swollen stack. Stratum corneum shows a much larger variation in swelling with the changes in relative humidity (Blank et al., 1984). This is most probably due to electrostatic double-layer repulsion, which is much more long ranged than the repulsive force F_r in Eq. 6 (Sparr and Wennerström, 2000).

SOLUTE FLUX

Diffusion of dissolved molecules

Water flux over the bilayer stack is determined by the physical state of the lipids and the boundary conditions, and it is not really affected by the swelling of the aqueous layers. When describing flux of small solute molecules, in contrast, it is no longer appropriate to neglect the gradient in chemical potential of the diffusing species across the water layer. The swelling of the lamellar phase therefore has to be included into the calculations. We have previously shown that, for a stack of one-phase bilayers, the steady-state diffusional flux through a nonhomogeneously swollen system is equal to the flux through a system consisting of one hydrocarbon layer and one aqueous layer of thickness $L_\alpha = \sum_1^{n_\alpha} l_\alpha$ and $H_\alpha = \sum_1^{n_\alpha} h_\alpha$, respectively (Sparr and Wennerström, 2000). The perpendicular flux of i through the one-phase bilayers in L_α and L_β state can analogously be derived to (cf. Sparr and Wennerström, 2000, Eq. 13),

$$J_i^\alpha = -D_i^\alpha \frac{L_\alpha + H_\alpha}{(L_\alpha + H_\alpha/K_{\alpha,i})(L_\alpha + H_\alpha K_{\alpha,i}(D_i^\alpha/D_i^w))}\Delta c_i^\alpha$$
$$= P_{eff,i}^\alpha \Delta c_i^\alpha, \quad \alpha = L_\alpha, L_\beta, \tag{22}$$

where $K_{\alpha,i}$ is the partition coefficient between the apolar part of the bilayer and the aqueous layers, and Δc_i^α is the concentration gradient of i over the α phase bilayers. D_i^w and D_i^α are the diffusions coefficients of i in the aqueous and hydrocarbon layers, respectively. Differences in the effective permeability, $P_{eff,i}$ between the different solutes i in a given phase is mainly caused by differences in the partition coefficient, $K_{\alpha,i}$.

For the two-phase bilayers, the situation is more complicated. From induction, an argument follows that the steady-state diffusional flux can be expressed as

$$J_i^{2\Phi} = -\left(\sum_{n=1}^{n_{2\Phi}} \frac{1}{P_{eff,i}^{2\Phi}(n)}\right)^{-1} \Delta c_i^{2\Phi}, \tag{23}$$

where

$$P_{eff,i}^{2\Phi}(n) = \left[A_{L_\alpha} X_{L_\alpha} \frac{D_i^{L_\alpha}(l_{L_\alpha} + h_{L_\alpha})}{(l_{L_\alpha} + h_{L_\alpha}/K_{L_\alpha,i})(l_{L_\alpha} + h_{L_\alpha} K_{L_\alpha,i}(D_i^{L_\alpha}/D_i^w))}\right.$$
$$\left. + A_{L_\beta} X_{L_\beta} \frac{K_{L_\beta,i}}{K_{L_\alpha,i}} \frac{D_i^{L_\beta}(l_{L_\beta} + h_{L_\beta})}{(l_{L_\beta} + h_{L_\beta}/K_{L_\beta,i})(l_{L_\beta} + h_{L_\beta} K_{L_\beta,i}(D_i^{L_\beta}/D_i^w))}\right]$$
$$\div (A_{L_\alpha} X_{L_\alpha} + A_{L_\beta} K_{L_\beta,i}/K_{L_\alpha,i}). \tag{24}$$

The values of X_α, h_α, and l_α depend on the layer, n. The solute flux over the L_α, L_β, and 2Φ bilayers are given by Eqs. 22–24. As described above, the number of bilayers in each state is determined by the gradient in water chemical potential. Consequently, the complete expression for solute flux is also dependent on the boundary conditions in water chemical potential. Under steady-state conditions, the solute

flux across each bilayer is equal, and $J_i = J_i^{L_\alpha} = J_i^{2\Phi} = J_i^{L_\beta}$, giving

$$J_i = \begin{cases} -P_{eff}^{L_\alpha}\Delta c_i, & \Delta\mu_w^B < \Delta\mu_w^{rh} \le \Delta\mu_w^{ref} \\ -\dfrac{P_{eff}^{L_\alpha}\left(\sum_n 1/P_{eff}^{2\Phi}(n)\right)^{-1}}{P_{eff}^{L_\alpha} + \left(\sum_n 1/P_{eff}^{2\Phi}(n)\right)^{-1}}\Delta c_i, & \Delta\mu_w^A < \Delta\mu_w^{rh} \le \Delta\mu_w^B \\ -\dfrac{P_{eff}^{L_\alpha}\left(\sum_n 1/P_{eff}^{2\Phi}(n)\right)^{-1}P_{eff}^{L_\beta}}{P_{eff}^{L_\alpha}\left(\sum_n 1/P_{eff}^{2\Phi}(n)\right)^{-1} + \left(\sum_n 1/P_{eff}^{2\Phi}(n)\right)^{-1}P_{eff}^{L_\beta} + P_{eff}^{L_\alpha}P_{eff}^{L_\beta}}\Delta c_i, & \Delta\mu_w^{rh} \le \Delta\mu_w^A, \end{cases} \quad (25)$$

where the effective permeability coefficients are defined in Eqs. 22 and 24. In Eq. 25, the gradient of the solute molecules is expressed as a gradient in the average concentration with respect to both the aqueous and the lipid regions. This is convenient if we want to study molecular transport within the lamellar stack without considering the surrounding phases. In contrast, if we want to study transport from a third phase, gas or solution, over the membrane, it is more convenient to utilize the chemical potential of species *i*, in analogy to the previous description of water transport, Eq. 14–16.

Solute flux through a responding membrane

For the description of transport of dissolved molecules, Fick's diffusion equation has to be solved for the whole system, including both the water and the lipid regions. Thus, not only the state of the lipids, but also the thickness of the aqueous layer and the lipid/water partition coefficients, K_α, have large influence on the permeability (Eqs. 22–25). It is clear that, for $K_\alpha \gg 1$ and $K_\alpha \ll 1$, i.e., when the solute strongly prefers one region relative to another, the perpendicular diffusion rate is strongly reduced. Experimental data on the difference in the partition coefficient between the gel and the liquid–crystalline lipids are very scarce. However, one can expect a higher solubility in a liquid phase than in a solid phase for most compounds. Fluorescence emission studies have shown considerably higher solubility of fluorescent amphiphilic molecules in liquid crystalline bilayers than in gel phase bilayers. An exception is when these themselves form a gel phase (Mesquita et al., 2000). The difference in partition coefficient between solid and fluid phases is also crucial for epifluorescence microscopy studies where solid condensed domains in lipid monolayers can be distinguished from the fluid-expanded domains due to the partition of the fluorescent probe into the liquid phases (McConnell, 1991). It is therefore reasonable to assume that the partition coefficient between the gel-phase lipids and water is considerably lower than the partition coefficient between liquid–crystalline lipids and water. This implies that the permeability coefficient changes substantially along the stack as the bilayers go through the phase transformations.

Figure 6 *A* shows the calculated flux of a solute *i* as a function of the boundary conditions of relative humidity for a constant gradient in solute concentration, Δc_i. It is obvious that the flux strongly depends on the boundary conditions. When all the bilayers are in liquid–crystalline state the permeability of the system decreases with increasing relative humidity. This is a consequence of the increased swelling and the longer diffusion pathway. At lower relative humidities at the boundary, $\Delta\mu_w^{rh} \le \Delta\mu_w^B$, the flux is dramatically reduced, due to the increased fraction of gel phase in the membrane. Finally, at boundary conditions of $\Delta\mu_w^{rh} \le \Delta\mu_w^A$ (the upper bilayers are in the gel state) the solute flux is about one order of magnitude lower compared to when $\Delta\mu_w^{rh} > \Delta\mu_w^B$ (all bilayers are in liquid–crystalline state). Increased permeability upon increasing humidity at the boundary has also been demonstrated for penetration through stratum corneum, in vivo (the so-called occlusion effect) (Roberts and Walker, 1993; Larsson, 1994). According to our model, this effect is caused by an increase in the boundary value of $\Delta\mu_w^{rh}$, which affects the gel–liquid-crystalline equilibrium of the stacked bilayers.

Figure 6 can be used to illustrate drug transport over the bilayer stack. In the numerical example, the partition coefficient between L_α hydrocarbon chains and the aqueous layers is set to 12, which is the tabulated value for the octanol/water partition coefficient of nicotine. The partition coefficient between L_β hydrocarbon chains and the aqueous layers is assumed to be 100 times lower. This implies that, when the bilayers are in the gel state, the solute molecules

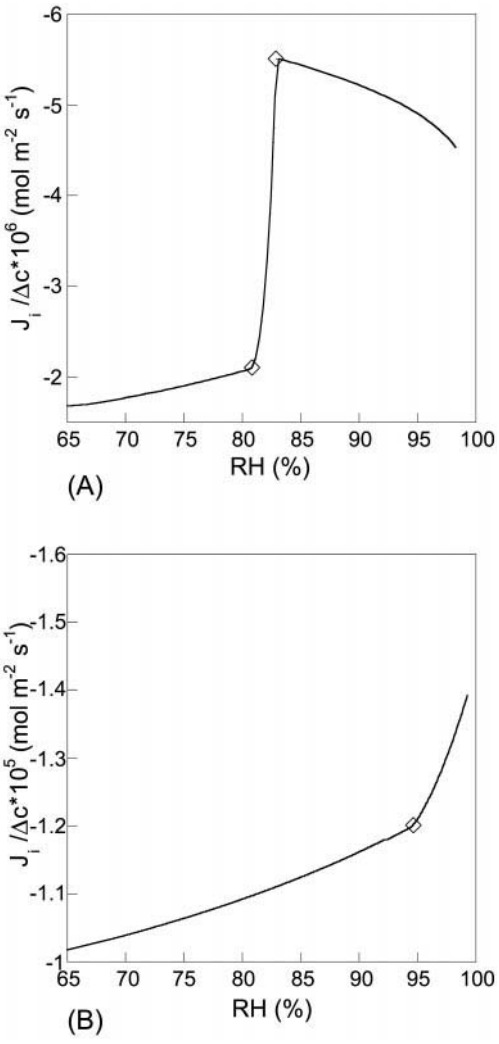

FIGURE 6 Calculated solute flux as a function of the relative humidity at the boundary. (*A*) Calculated flux through a DLPC–DMPC ($X_{\mathrm{DMPC}} = 0.5$) membrane ($T = 30$°C). (*B*) Calculated flux through a DLPC–DPPC ($X_{\mathrm{DPPC}} = 0.75$) membrane. The partition coefficients are set to $K_{\mathrm{i}}^{\mathrm{L}\text{-}\alpha} = 12$ and $K_{\mathrm{i}}^{\mathrm{L}\text{-}\beta} = 0.12$, and diffusion coefficients are assumed to be $D_{\mathrm{i}}^{\mathrm{L}\text{-}\alpha} = D_{\mathrm{i}}^{\mathrm{w}} = 1 \times 10^{-9}$ m/s and $D_{\mathrm{i}}^{\mathrm{L}\text{-}\beta} = 1 \times 10^{-11}$ m/s. $K_{\mathrm{i}}^{\mathrm{L}\text{-}\alpha}$ is the tabulated value for the octanol/water partition coefficient of nicotine. The diamonds indicate $\Delta\mu_{\mathrm{w}}^{\mathrm{A}}$ and $\Delta\mu_{\mathrm{w}}^{\mathrm{B}}$ phase boundaries where the upper bilayer goes through the transitions (*A*) (L_α–2Φ) and (*A*, *B*) (2Φ–L_β). $T = 30$°C.

have a higher partition to the aqueous domains, whereas, when the bilayers are in the liquid–crystalline state, the solute molecules prefer the hydrocarbon regions. The nonlinear response in the flux is a combined effect of variations of mobility and partition of the solute molecule along the gradient. In other words, the demonstrated transport behavior is not only an effect from the phase transformations and the swelling, but also an effect of the variation in partition coefficient between the bilayers and the aqueous layers along the gradient in $\Delta\mu_{\mathrm{w}}$.

At the present stage, we have made the assumption that the dissolved molecules are of a relatively low concentration and do not influence the phase behavior in a major way. In many applications of transdermal drug delivery, the dosage of an applied substance is very high, and it can affect the bilayer phase behavior along the solute concentration gradient. If the solute substance has a higher solubility in the liquid–crystalline phase than in the gel phase, a phase transition can be induced along the solute gradient according to the same mechanism as for water. This offers another route to influence the membrane permeability. Incorporating this mechanism into the model leads to an additional coupling of water and solute fluxes.

In the numerical calculations, the diffusion coefficients in the aqueous and in the fluid chains of the liquid–crystalline bilayers was assumed to be equal, $D_{\mathrm{i}}^{\mathrm{L}\text{-}\alpha} \approx D_{\mathrm{i}}^{\mathrm{w}}$. This assumption is supported by computer simulations on diffusion over a liquid–crystalline bilayer showing that the diffusion coefficients of water and solutes are of the same order of magnitude in the aqueous layers and in the hydrocarbon chain part of the bilayers (Marrink and Berendsen, 1994, 1996). Allowing for $D_{\mathrm{i}}^{\mathrm{L}\text{-}\alpha} \neq D_{\mathrm{i}}^{\mathrm{w}}$, within reasonable limits, will affect the results quantitatively but not the qualitative picture. Experimental and theoretical data for diffusion over gel-phase bilayers is more scarce. Diffusion experiments in vesicles suggest that the permeability coefficient in the gel-state bilayers is at least two orders of magnitude lower than in the liquid-crystalline bilayers (Lawaczeck, 1979; Xiang and Anderson, 1998).

So far, we have only considered the case where the whole bilayers in the lower parts of the stack ($z = 0$) are in the L_α state. Figure 6 *B* illustrates the solute flux through a membrane of DLPC–DPPC, $X_{\mathrm{DPPC}} = 0.75$ at 30°C. According to the phase diagram (Fig. 1 *B*, nonideal case) only a small fraction of the lipids are in the liquid-crystalline L_α state at $\Delta\mu_{\mathrm{w}} = \Delta\mu_{\mathrm{w}}^{\mathrm{ref}}$. Still, it is clearly shown that the membrane permeability is strongly increased for high relative humidities at the boundary. This example illustrates that even the presence of a small amount of liquid–crystalline phase has a profound effect on the membrane properties, particularly at high relative humidity at the boundary. This is a circumstance highly relevant for the conditions in the stratum corneum.

Lipids strongly respond to changes in their environment. Small changes in lipid composition, water content, pH, temperature, etc., can affect the arrangement of fluid and solid domains and can thereby change the permeability. This implies that the permeability can be varied in a controlled and determined way by changing some external variables. The lamellar structure of stratum corneum provides an effective barrier to passive diffusion of small molecules and prevents the body from uncontrolled water loss. There exists a huge literature on methods for enhancing the permeability to develop effective drug delivery systems (Potts et al., 1991; Johnson et al., 1996). It is, for example, shown that inclusion of fatty acids in transdermal formulations enhances the permeability of a wide range of

compounds over skin. The enhancing effect is most dominant for fatty acids with low melting points, like oleic acid and lauric acid. (Francoeur et al., 1990; Mandal and Downing, 1993; Smith and Anderson, 1995). One suggested mechanism for the enhanced permeability is that the fluid fatty acid is incorporated into the stratum corneum lipid bilayer, inducing a greater fraction of fluid domains and thus facilitating diffusion (Potts et al., 1991). In the perspective of the present model, this is comparable to the effect shown in Fig. 6 *B*, where incorporation of a small fraction of a fluid lipid into a gel-forming bilayer results in an increased permeability. Enhanced permeability upon addition of free fatty acids has also been demonstrated for phospholipid vesicles (Langner and Hui, 2000).

The permeability of the gel-phase bilayers is much lower than the permeability of the liquid–crystalline bilayers. In the present model, the permeability of the two-phase bilayers is basically determined as the weighted average of the effective permeability of the gel and the liquid–crystalline bilayers. However, several studies have demonstrated an increased solute permeability in bilayers in the two-phase gel–liquid-crystalline coexistence regions (Blok et al., 1975; Cruzeiro-Hansson and Mouritsen, 1988; Clerc and Thompson, 1995; Xiang and Anderson, 1998). This phenomenon can be attributed to an increase in permeability at the domain boundaries. One molecular explanation for this can be an accumulation of a line-active (compare surface-active) substance, the solute itself or a bilayer component, along the domain boundaries, resulting in a different composition and a higher permeability in these regions. Line-active properties have been demonstrated for, e.g., cholesterol (Weis and McConnell, 1985; Sparr et al., 1999). At the present stage, special effects at the domains boundaries are not incorporated into the model. The calculated results for solute and water flux through a bilayer stack where some of the bilayers are in the two-phase gel–liquid-crystalline coexistence region can therefore be underestimated.

In deriving the expression for perpendicular diffusion over the bilayer stack, the lateral diffusion in the membrane, i.e., the diffusion parallel to the stack, is neglected. This is not a restrictive assumption in the cases of one-phase bilayers. In the two-phase bilayers, in contrast, the neglect of the lateral transport of solute molecules is more problematic. In the present model, the flux over the two-phase region is calculated as the weighted flux over the two phases, based on the area fraction occupied by each phase (Eqs. 16 and 24). A physical interpretation of this assumption is that the domains of gel and liquid–crystalline phases are very small and the lateral diffusion pathway is regarded negligible. No experimental data on domain size in the bilayers of the stratum corneum lipid matrix are available from the literature. However, atomic force microscopy studies on monolayers of model stratum corneum lipids show domain formation in the nanometer range (ten Grotenhuis et al., 1996; Sparr et al., 2001). Domains in the length scale of 10 nm have also been observed by atomic force microscopy in monolayers of DMPC and DSPC (Gliss et al., 1998). Furthermore, lateral domain organization in the nanometer range in phospholipid bilayers is predicted from computer simulations (Mouritsen and Jørgensen, 1998) and from various experimental results (Mouritsen and Jørgensen, 1997). In the case of nanometer lateral segregation in the bilayers, the tortuous diffusion pathway due to domain formation can be considered negligible, and lateral diffusion can therefore be neglected.

CONCLUSIONS

We have presented a model for describing the influence of a gradient in water chemical potential on the transport and phase behavior in a stack of lipid bilayers. Phase behavior of binary phospholipid mixtures at varying osmotic pressures (water chemical potentials) are modeled on the basis of regular solution theory and known interlamellar forces. Previous experimental and theoretical studies of single phospholipid–water systems have shown that a phase transition from a liquid–crystalline to a gel phase can be triggered by an increase of the osmotic pressure (isothermal conditions) (Ulmius et al., 1977; Janiak et al., 1979; Smith et al., 1990; Markova et al., 2000). In the binary phospholipid phase diagram a two-phase coexistence region is induced between the liquid–crystalline and the gel phases. The Π_{osm}–X phase diagrams closely resemble the corresponding T–X phase diagram in excess water (Shimshick and McConnell, 1973). This shows that variation in different intensive variables causes similar response in the phase behavior.

From the known equilibrium phase behavior in a homogenous mixture, it is possible to predict the phase equilibria in a bilayer stack in the presence of a gradient in water chemical potential. The local water chemical potential determines the local lipid-phase behavior. The structural transformations along the gradient result in a nonlinear transport behavior, where the nonlinearity can be attributed to changes in both the lipid (phase transformations) and the aqueous (swelling) regions. For a binary phospholipid bilayer stack, transitions from liquid–crystalline to gel-state bilayers can be induced by decreasing the water chemical potential at the boundary. The calculations show that even a very small fraction of gel bilayers gives a dramatic reduction of the membrane permeability. This results in a leveling off in water flux and a decrease in solute flux. A control of the boundary conditions in water chemical potential can thus be used as a switch for the membrane permeability.

The main source of inspiration for this model is the extracellular lipids in stratum corneum, the outer layer of skin. In the present paper, calculations were performed for binary phospholipid membranes, although these are not typical stratum corneum lipids. The reason for this is that phospholipids are well-studied systems and most of the experimental data needed for doing quantitative interpreta-

tions can be obtained from the literature. However, in comparison with skin, it can be noted that phase transformations from a liquid–crystalline state to a gel state at decreasing water contents have also been demonstrated for stratum corneum lipids (Gay et al., 1994; Shah et al., 1995).

The relation between the gradient in water chemical potential and the experimentally determined water flux over skin (Blank et al., 1984) is consistent with the calculations (Fig. 4). This suggests that the mechanism described in the present model is also a mechanism operating for the skin lipids. In the case of solute flux, it is shown that the membrane permeability can be enhanced by an increase of the water chemical potential at the boundary (the so-called occlusion effect) and by incorporation of fluid state lipids in the bilayers. Solute flux is also strongly dependent on the partition coefficients between the liquid crystalline, gel, and aqueous layers. Most substances rather partition into a liquid–crystalline bilayer than into a gel one. A gradient in water chemical potential can therefore introduce a gradient in partition between the bilayers and the aqueous layers along the membrane. A high partition of the solute to liquid crystalline bilayers can also trigger phase transitions along the gradient in solute chemical potential, according to the same mechanism as here described for water.

In all calculations of diffusional flux, we have made the restrictive assumptions that the diffusion coefficients and the partition coefficients are uniform in each aqueous and lipid layer and that the interfacial resistance is negligible. This implies that the bilayers are treated as homogenous. However, in a more detailed description, the inhomogenities within the bilayers should also be considered. Computer simulations on diffusion through phospholipid bilayers have shown that the diffusion rate is lower in the interfacial regions compared to the aqueous layers and the central parts of the bilayers (Marrink and Berendsen, 1994, 1996). Thus, for a more complete description, the interfacial regions should also be incorporated as separate layers in the model. This effect would change the quantitative results, although the general description and the trends are still the same.

This work was supported by the Swedish Natural Science Research Council.

REFERENCES

Blank, I. H., J. Moloney, A. G. Emslie, I. Simon, and C. Apt. 1984. The diffusion of water across the stratum corneum as a function of its water content. *J. Invest. Dermatol.* 82:188–194.

Blok, M. C., E. C. M. Van der Neut-Kok, L. L. M. van Deenen, and J. de Gier. 1975. The effect of chain length and lipid phase transition on the selective properties of liposomes. *Biochim. Biophys. Acta.* 406:187–196.

Bloom, M., E. Evans, and O. G. Mouritsen. 1991. Physical properties of the fluid lipid-bilayer component of cell membranes: a perspective. *Quart. Rev. Biophys.* 24:293–397.

Boddé, H. E., I. van der Brink, H. K. Koerten, and F. H. N. de Hann. 1991. Visualization of in vitro percutaneous penetration of mercuric chloride; Transport through intercellular space versus cellular uptake through desmosomes. *J. Control. Release.* 15:227–236.

Bouwstra, J. A., G. S. Gooris, M. A. Salomons-De Vries, J. A. van der Spek, and W. Bras. 1992. Structure of human stratum corneum as a function of temperature and hydration: A wide-angle x-ray diffraction study. *Int. J. Pharm.* 84:205–216.

Cevc, G. 1993. *Phospholipids Handbook.* Marcel Dekker, Inc., New York. 935–951.

Clerc, S. G., and T. E. Thompson. 1995. Permeability of dimyristoyl phosphatidylcholine/dipalmitoyl phosphatidylcholine bilayer-membranes with coexisting gel and liquid-crystalline phases. *Biophys. J.* 68:2333–2341.

Cruzeiro-Hansson, L., and O. G. Mouritsen. 1988. Passive ion transport of liquid membranes modelled via lipid-domain interfacial area. *Biochim. Biophys. Acta.* 944:63–72.

Davis, A. D., T. M. Weatherby, D. K. Hartline, and P. H. Lenz. 1999. Myelin-like sheaths in copepod axons. *Nature.* 398:571–571.

De Wit, A. 1999. *Spatial Patterns and Spatiotemporal Dynamics in Chemical Systems.* I. Prigofine, S. Rice (editors). John Wiley & Sons, Inc., New York. 435–513.

Dratz, E. A., and P. A. Hargrave. 1983. The structure of rhodopsin and the rod outer segment disk membrane. *Trends Biochem. Sci.* 8:128–131.

Elias, P. M. 1991. Epidermal barrier function: intercellular epidermal lipid structures, origin, composition and metabolism. *J. Control. Release.* 15:199–208.

Engelbert, H. P., and R. Lawaczeck. 1985. The H_2O/D_2O exchange across vesicular lipid bilayers. Lecithins and binary mixtures of lecithins. *Ber. Bunsenges. Phys. Chem.* 89:754–759.

Evans, D. F., and H. Wennerström. 1999. *The Colloidal Domain, Where Physics, Chemistry and Biology Meet.* Chap. 1. 2nd ed. VCH Publishers, Inc., New York. 1–43.

Falla, W. R., M. Mulski, and E. L. Cussler. 1996. Estimating diffusion through flake-filled membranes. *J. Membr. Sci.* 119:129–138.

Forslind, B. 1994. A domain mosaic model of the skin barrier. *Acta Derm. Venerol.* 74:1–6.

Francoeur, M. L., G. M. Golden, and R. O. Potts. 1990. Oleic-acid—its effects on stratum-corneum in relation to (trans)dermal drug delivery. *Pharm. Res.* 7:621–627.

Gabriella-Madelmont, C., and R. Perron. 1983. Calorimetric studies on phospholipid–water systems. I. DL-dipalmitoylphosphatidylcholine (DPPC) - water system. *J. Coll. Interface Sci.* 95:471–482.

Gay, C. L., R. H. Guy, G. M. Golden, V. H. W. Mak, and M. L. Francoeur. 1994. Characterization of low-temperature (ie, less-than-65 degrees C) lipid transitions in human stratum-corneum. *J. Invest. Dermatol.* 103: 233–239.

Gliss, C., H. Clausen-Schaumann, R. Günther, S. Odenbach, O. Randl, and T. M. Bayerl. 1998. Direct detection of domains in phospholipid bilayers by grazing incidence diffraction of neutrons and atomic force microscopy. *Biophys. J.* 74:2443–2450.

Graziani, Y., and A. Livne. 1972. Water permeability of bilayer lipid membranes. Sterol-lipid interaction. *J. Membr. Biol.* 7:275–284.

Guldbrand, L., B. Jönsson, and H. Wennerström. 1982. Hydration forces and phase equilibria in the dipalmitoyl phosphatidylcholine-water system. *J. Colloid Interf. Sci.* 89:532–541.

Hatcher, M. E., and W. Z. Plachy. 1993. Dioxygen diffusion in the stratum-corneum - an EPR spin-label study. *Biochim. Biophys. Acta* 1149:73–78.

Hui, S. W., T. L. Kuhl, Y. Q. Guo, and J. Israelachvili. 1999. Use of poly(ethylene glycol) to control cell aggregation and fusion. *Colloid Surf. B-Biointerfaces.* 14:213–222.

Ipsen, J. H., and O. G. Mouritsen. 1988. Modelling the phase-equilibria in 2-component membranes of phospholipids with different acyl-chain lengths. *Biochim. Biophys. Acta.* 944:121–134.

Israelachvili, J. 1992. *Intermolecular and Surface Forces.* 2nd ed. Academic Press Ltd., London.

Israelachvili, J., and H. Wennerström. 1992. Entropic forces between amphiphilic surfaces in liquids. *J. Phys. Chem.* 96:520–531.

Janiak, M. J., D. M. Small, and G. G. Shipley. 1979. Temperature and compositional dependence of the structure of hydrated dimyrisoyl lecithin. *J. Biol. Chem.* 254:6068–6078.

Johnson, M. E., S. Mitragotri, A. Patel, D. Blankschtein, and R. Langer. 1996. Synergistic effects of chemical enhancers and therapeutic ultrasound on transdermal drug delivery. *J. Pharm. Sci.* 85:670–679.

Kitson, N., and J. L. Thewalt. 2000. Hypothesis: The epidermal permeability barrier is a porous medium. *Acta Derm. Venerol.* 12–15.

Landh, T. 1996. Cubic cell membrane architectures. PhD Thesis, Lund University, Sweden.

Langner, M., and S. W. Hui. 2000. Effect of free fatty acids on the permeability of 1,2-dimyristoyl-*sn*-glycero-3-phosphocholine bilayer at the main phase transition. *Biochim. Biophys. Acta.* 1463:439–447.

Larsson, K. 1994. Lipids—molecular Organization, Physical Functions and Technical Applications. Chap. 11. Oily Press Ltd. Dundee, Scotland. 147–153.

Lawaczeck, R. 1979. On the permeability of water molecules across vesicular bilayers. *J. Membr. Biol.* 51:229–261.

Lis, L. J., M. McAlister, N. Fuller, R. P. Rand, and V. A. Parsegian. 1982a. Interactions between neutral phospholipid bilayer membranes. *Biophys. J.* 37:657–666.

Lis, L. J., M. McAlister, N. Fuller, R. P. Rand, and V. A. Parsegian. 1982b. Measurement of the lateral compressibility of several phospholipid bilayers. *Biophys. J.* 37:667–672.

Mabrey, S., and J. M. Sturtevant. 1976. Investigation of phase transitions of lipids and lipid mixtures by high sensitivity differential scanning calorimetry. *Proc. Natl. Acad. Sci. U.S.A.* 73:3862–3866.

Mandal, T. K., and D. T. Downing. 1993. Freeze-fracture electron-microscopic and osmotic water permeability studies of epidermal lipid liposomes derived from stratum-corneum lipids of porcine epidermis. *Acta Derm. Venereol.* 73:12–17.

Markova, N., E. Sparr, L. Wadsö, and H. Wennerström. 2000. A calorimetric study of phospholipid hydration. Simultaneous monitoring of enthalpy and free energy. *J. Phys. Chem. B.* 104:8053–8060.

Marrink, S. J., and H. J. C. Berendsen. 1994. Simulation of water transport through a lipid membrane. *J. Phys. Chem.* 98:4155–4168.

Marrink, S. J., and H. J. C. Berendsen. 1996. Permeation process of small molecules across lipid membranes studied by molecular dynamics simulations. *J. Phys. Chem.* 100:16729–16738.

McConnell, H. M. 1991. Structures and transitions in lipid monolayers at the air–water interface. *Annu. Rev. Phys. Chem.* 42:171–195.

Mesquita, R., E. Melo, T. E. Thompson, and W. L. C. Vaz. 2000. Partitioning of amphiphiles between coexisting ordered and disordered phases in two-phase lipid bilayer membranes. *Biophys. J.* 78: 3019–3025.

Mouritsen, O. G., and K. Jørgensen. 1997. Small-scale lipid-membrane structure: simulation versus experiment. *Curr. Opin. Struct. Biol.* 7:518–527.

Mouritsen, O. G., and K. Jørgensen. 1998. A new look at lipid-membrane structure in relation to drug research. *Pharm. Res.* 15:1507–1519.

Norlén, L., I. Nicander, A. Lundsjö, T. Cronholm, and B. Forslind. 1998. A new HPLC-based method for the quantitative analysis of inner stratum corneum lipids with special reference to the free fatty acid fraction. *Arch. Dermatol. Res.* 290:508–516.

Parsegian, V. A., N. Fuller, and R. P. Rand. 1979. Measured work of deformation and repulsion of lecithin bilayers. *Proc. Natl. Acad. Sci. U.S.A.* 76:2750–2754.

Potts, R. O., and M. L. Francouer. 1990. Lipid biophysics of water loss through the skin. *Proc. Natl. Acad. Sci. U.S.A.* 87:3871–3873.

Potts, R. O., V. H. Mak, R. H. Guy, and M. L. Francoeur. 1991. Strategies to enhance permeability via stratum corneum lipid pathways. *Adv. Lipid Res.* 24:175–212.

Rand, R. P., and V. A. Parsegian. 1989. Hydration forces between phospholipid bilayers. *Biochim. Biophys. Acta.* 988:351–376.

Rietveld, A., and K. Simons. 1998. The differential miscibility of lipids as the basis for the formation of functional membrane rafts. *Biochem. Biophys. Acta.* 1376:467–479.

Roberts, M. S., and M. Walker. 1993. Water: The Most Natural Penetration Enhancer. K. A. Walters, J. Hadgraft, editors. Marcel Dekker, New York. 1–30.

Shah, J., J. M. Atienza, A. V. Rawlings, and G. G. Shipley. 1995. Physical-properties of ceramides—effect of fatty-acid hydroxylation. *J. Lipid Res.* 36:1945–1955.

Shimshick, E. J., and H. M. McConnell. 1973. Lateral phase separation in phospholipid membranes. *Biochemistry.* 12:2351–2360.

Smith, G. S., E. B. Sirota, C. R. Safinya, R. J. Plano, and N. A. Clark. 1990. X-ray structural studies of freely suspended ordered hydrated DMPC multimembrane films. *J. Chem. Phys.* 92:4519–4529.

Smith, S. W., and B. D. Anderson. 1995. Human skin permeability enhancement by lauric acid under equilibrium aqueous conditions. *J. Pharm. Sci.* 84:551–556.

Sparr, E., K. Ekelund, J. Engblom, S. Engström, and H. Wennerström. 1999. An AFM study of lipid monolayers: II. The effect of cholesterol on fatty acids. *Langmuir.* 15:6950–6955.

Sparr, E., L. Eriksson, J. A. Bouwstra, and K. Ekelund. 2001. AFM study of lipid monolayers: III. Phase behavior of ceramides, cholesterol and fatty acids. *Langmuir.* 17:164–172.

Sparr, E., and H. Wennerström. 2000. Diffusion through a responding lamellar liquid crystal. A model of molecular transport across stratum corneum. *Colloids Surf. B-Biointerfaces.* 19:103–116.

Steponkus, P. L. 1999. Freeze-Induced Dehydration and the Cryostability of Biological Membranes. Y. H. Poos, R. B. Leslie, P. J. Lillford, editors. Technomic Publishing Co. Inc., Lancaster. Basel, Switzerland.

Sugar, I. P., T. E. Thompson, and R. L. Biltonen. 1999. Monte Carlo simulation of two-component bilayers: DMPC/DSPC mixtures. *Biophys. J.* 76:2099–2110.

ten Grotenhuis, E., R. A. Demel, M. Ponec, D. R. Boer, J. C. van Miltenburg, and J. A. Bouwstra. 1996. Phase behavior of stratum corneum lipids in mixed Langmuir–Blodgett monolayers. *Biophys. J.* 71: 1389–1399.

Ulmius, J., H. Wennerström, B. Lindblom, and G. Arvidson. 1977. Deuteron nuclear magnetic resonance studies of phase equilibria in a lecithin–water system. *Biochemistry.* 16:5742–5745.

Weis, R. M., and H. M. McConnell. 1985. Cholesterol stabilizes the crystal–liquid interface in phospholipid monolayers. *J. Phys. Chem.* 89:4453–4459.

Wertz, P. W., D. C. Swartzendruber, K. C. Madison, and D. T. Downing. 1987. Composition and morphology of epidermal cyst lipids. *J. Invest. Dermatol.* 89:419–425.

White, S. H., D. Mirejovsky, and G. I. King. 1988. Structure of lamellar lipid domains and corneocyte envelopes of murine stratum-corneum—a x-ray diffraction study. *Biochemistry.* 27:3725–3732.

Xiang, T. X., and B. D. Anderson. 1998. Phase structures of binary lipid bilayers as revealed by permeability of small molecules. *Biochim. Biophys. Acta.* 1370:64–76.